

The Analysis of Large Order Bessel Functions in Gravitational Wave Signals from Pulsars

F. A. Chishtie^{1,3}, S. R. Valluri^{1,2,4}, K. M. Rao¹, D. Sikorski² and T. Williams²

¹Department of Applied Mathematics,
University of Western Ontario, London, ON N6A 5B7

²Department of Physics and Astronomy,
University of Western Ontario, London, ON N6A 3K7

Email: ³fchishti@uwo.ca

Email: ⁴valluri@uwo.ca

Abstract

In this work, we present the analytic treatment of the large order Bessel functions that arise in the Fourier Transform (FT) of the Gravitational Wave (GW) signal from a pulsar. We outline several strategies which employ asymptotic expansions in evaluation of such Bessel functions which also happen to have large argument. Large order Bessel functions also arise in the Peters-Mathews model of binary inspiralling stars emitting GW and several problems in potential scattering theory. Other applications also arise in a variety of problems in Applied Mathematics as well as in the Natural Sciences and present a challenge for High Performance Computing(HPC).

1. Introduction

The detection of gravitational waves (GW) from astrophysical sources is one of the most outstanding problems in experimental gravitation today. Large laser interferometric gravitational wave detectors like the LIGO, VIRGO, LISA, TAMA 300, GEO 600 and AIGO are potentially opening a new window for the study of a vast and rich variety of nonlinear curvature phenomena.

In recent works [1] we have analyzed the Fourier transform (FT) of the Doppler shifted GW signal from a pulsar with the use of the Plane Wave Expansion in Spherical Harmonics (PWESH). Spherical-harmonic multipole expansions are used throughout theoretical physics. The expansion of a plane wave in spherical harmonics has a variety of applications not only in quantum mechanics and electromagnetic theory [2], but also

in many other areas. A number of researchers have used spherical-harmonic expansions for a variety of problems in general relativity, including problems where nonlinearity shows up[3]. The basis states in the PWESH expansion form a complete set and facilitate such a study. It also turns out that the consequent analysis of the Fourier Transform (FT) of the GW signal from a pulsar has a very interesting and convenient development in terms of the resulting spherical Bessel, generalized hypergeometric function, the Gamma functions and the Legendre functions. Both rotational and orbital motions of the Earth and spindown of the pulsar can be considered in this analysis which happens to have a nice analytic representation for the GW signal in terms of the above special functions. The signal can then be studied as a function of a variety of different parameters associated with both the GW pulsar signal as well as the orbital and rotational parameters. The numerical analysis of this analytical expression for the signal offers a challenge for fast and high performance parallel computation. The plane wave expansion approach was also used by Bruce Allen and Adrian C. Ottewill [4] in their study of the correlation of GW signals from ground-based GW detectors. They use the correlation to search for anisotropies from stochastic background in terms of the l, m multipole moments. Our PWESH formalism enables a similar study. Recent studies of the Cosmic Microwave Background Explorer have raised the interesting question of the study of very large multipole moments with angular momentum l and its projection m going up to very large values of $l \sim 1000$. Such problems warrant an intensive analytic study supplemented by numerical and parallel computation.

Since our FT depends on the Bessel function, a com-

putational issue arises due to large values of the index or order n of the function. In the GW form of the pulsar, the Doppler shifted orbiting motion gives rise to Bessel functions $J_n\left(\frac{2\pi f_0 A \sin \theta}{c}\right)$, where $\frac{2\pi f_0 A \sin \theta}{c}$ is large for non-negligible angle θ as is shown in the following section. Even for $\sin \theta \sim \frac{1}{1000}$, the argument is large necessitating the consideration of large values of n . The motivation of this work, is to extend the analysis in Watson [5] for large index, argument and overlapping situations. Meissel [6] has made derivations for large order Bessel functions both when the argument is smaller than the order and vice versa. The asymptotics of these large order Bessel functions are tricky in the sense that one runs into so-called ‘‘transition’’ regions where such expansions fail. These regions are values of the function when the argument is close to the given order. As an application, we will address the phenomenological situation of GW signal analysis of large order n (which does arise with combinations of l and m) and supplement the related computations with the presently derived results in a forthcoming paper.

Captures of stellar-mass compact objects (CO) by massive black holes are important capture sources for the Laser Interferometer Space Antenna (LISA), the space based GW detector due to be launched in about a decade[7]. Higher Harmonics of the orbital frequency of the COs arise in the post Newtonian (PN) capture GW model forms and contribute considerably to the total signal to noise (S/N) ratio of the waveform. The GW form can be decomposed into gravitational multipole moments which are treated in the Fourier analysis of Keplerian eccentric orbits. The radiation depends strongly on the orbital eccentricity e , and Bessel functions $J_n(ne)$ are a natural consequence of the analysis.

The calculation of partial derivatives of the potential scattering phase shifts which often contain Bessel and Legendre functions of large order angular momentum l , with respect to angular momentum arise in a variety of scattering problems in atomic, molecular and nuclear physics. In particular, large values of l can arise in rainbow, glory and orbit scattering. The analysis in our paper should help provide suitable approximations for large order and/or argument for the Bessel functions that arise in such problems.

2. Fourier Transform of the GW signal

The FT for the GW Doppler shifted pulsar signal [1] is given as follows:

$$\tilde{h}(f) = S_{nlm}(\omega_0, \omega_{orb}, T_{rE}, n, l, m, A, R, k, \alpha, \theta, \phi) =$$

$$\sum_{n=-\infty}^{\infty} \sum_{l=0}^{\infty} \sum_{m=-l}^l \psi_0 \psi_1 \psi_2 \psi_3 \psi_4 \quad (1)$$

where

$$\psi_0(n, l, m, \alpha, \theta, \phi) = 4\pi i^l Y_{lm}(\theta, \phi) N_{lm} P_l^m(\cos \alpha) \quad (2)$$

$$\begin{aligned} \psi_1(n, \theta, \phi, T_{rE}, f_0, A) &= T_{rE} \sqrt{\frac{\pi}{2}} e^{-i \frac{2\pi f_0 A}{c} \sin \theta \cos \phi} i^n e^{-in\phi} \\ &\times J_n\left(\frac{2\pi f_0 A \sin \theta}{c}\right) \end{aligned} \quad (3)$$

$$\psi_2(l, \omega_{orb}, \omega_r, n, m, R) = \left\{ \frac{1 - e^{i\pi(l - B_{orb})R}}{1 - e^{i\pi(l - B_{orb})}} \right\} \frac{e^{-iB_{orb} \frac{\pi}{2}}}{2^{2l}} \quad (4)$$

$$\begin{aligned} \psi_3(k, l, m, n, \omega_{orb}, \omega_r) &= k^{l+\frac{1}{2}} \\ &\times \frac{\Gamma(l+1)}{\Gamma\left(l+\frac{3}{2}\right) \Gamma\left(\frac{l+B_{orb}+2}{2}\right) \Gamma\left(\frac{l-B_{orb}+2}{2}\right)} \end{aligned} \quad (5)$$

$$\begin{aligned} \psi_4(k, l, m, n, \omega_{orb}, \omega_r) &= {}_1F_3\left(l+1; l+\frac{3}{2}, \right. \\ &\left. \frac{l+B_{orb}+2}{2}, \frac{l-B_{orb}+2}{2}; \frac{-k^2}{16}\right) \end{aligned} \quad (6)$$

The angle α is the co-latitude detector angle and angles θ, ϕ are associated with the pulsar source. Here $\omega_0 = 2\pi f_0$, $\omega_{orb} = \frac{2\pi}{T_{orb}}$ ($T_{orb} = 365$ days, $T_{rE} = 1$ day), $B_{orb} = 2\left(\frac{\omega - \omega_0}{\omega_r} + \frac{m}{2} + \frac{n\omega_{orb}}{\omega_{rot}}\right)$, $k = \frac{4\pi f_0 R_E \sin(\alpha)}{c}$ (R_E is the radius of Earth, c is the velocity of light) and $A = 1.5 \times 10^{11}$ meters is the sun-earth distance.

3. Extensions of Meissel’s and Steepest Descent Expansions

The Bessel function, of the type, $J_\nu(x)$ obeys the following differential equation [5],

$$z^2 \frac{d^2 J_\nu(\nu z)}{dz^2} + z \frac{dJ_\nu(\nu z)}{dz} + \nu^2(1 - z^2)J_\nu(\nu z) = 0 \quad (7)$$

where the argument x is parameterized by νz . If a function $u(z)$ is introduced such that

$$J_\nu(\nu z) = \frac{\nu^\nu}{\Gamma(\nu+1)} \exp\left\{\int^z u(z) dz\right\} \quad (8)$$

where $u(z)$ is a series in descending powers of ν ,

$$u(z) = \nu u_0 + u_1 + \frac{u_2}{\nu} + \frac{u_3}{\nu^2} + \frac{u_4}{\nu^3} + \frac{u_5}{\nu^4} + \frac{u_6}{\nu^5} + \frac{u_7}{\nu^6} + \frac{u_8}{\nu^7} + \frac{u_9}{\nu^8} + \dots \quad (9)$$

Substitution of this series and equation (8) in the differential equation (7) yields the following expressions for $u_i(z)$, $i = 0 \dots 5$,

$$\begin{aligned} u_0 &= \frac{\sqrt{1-z^2}}{z}, u_1 = \frac{z}{2(1-z^2)}, u_2 = -\frac{4z+z^2}{8(1-z^2)^{5/2}} \\ u_3 &= \frac{4z+10z^3+z^5}{8(1-z^2)^4}, u_4 = -\frac{64z+560z^3+456z^5+25z^7}{128(1-z^2)^{11/2}} \\ u_5 &= \frac{16z+368z^3+924z^5+347z^7+13z^9}{32(1-z^2)^7} \end{aligned}$$

Hence, by integrating u_i , and substituting in Equation (8) we arrive at Meissel's *First* expansion [6], which is valid for the case when the argument is less than the order ν . We do not list u_6, u_7, u_8 and u_9 as one can obtain these straightforwardly from their respective integrals shown below. These results are expressed as,

$$J_\nu(\nu z) = \frac{(\nu z)^\nu \exp(\nu\sqrt{1-z^2}) \exp(-V_\nu)}{e^\nu \Gamma(\nu+1)(1-z^2)^{1/4} [1+\sqrt{1-z^2}]^\nu} \quad (10)$$

where,

$$V_\nu = V_1 + V_2 + V_3 + V_4 + V_5 + V_6 + V_7 + V_8 + \dots \quad (11)$$

and,

$$V_1 = \frac{1}{24\nu} \left(\frac{2+3z^2}{(1-z^2)^{3/2}} - 2 \right), V_2 = -\frac{4z^2+z^4}{16\nu^2(1-z^2)^3}$$

$$V_3 = -\frac{1}{5760\nu^3} \left(\frac{16-1512z^2-3654z^4-375z^6}{(1-z^2)^{9/2}} - 16 \right)$$

$$V_4 = -\frac{32z^2+288z^4+232z^6+13z^8}{128\nu^4(1-z^2)^6}$$

$$V_5 = -\frac{1}{322560\nu^5(1-z^2)^{15/2}} (67599z^{10} + 1914210z^8 + 4744640z^6 + 1891200z^4 + 78720z^2 + 256) + \frac{1}{1260\nu^5}$$

$$V_6 = \frac{z^2}{192(1-z^2)^9\nu^6} (48+2580z^2+14884z^4 + 17493z^6+4242z^8+103z^{10})$$

$$\begin{aligned} V_7 &= -\frac{(1-z^2)^{-21/2}}{3440640\nu^7} (881664z^2 + 99783936z^4 \\ &+ 1135145088z^6 + 2884531440z^8 + 1965889800z^{10} \\ &+ 318291750z^{12} + 5635995z^{14} - 2048) - \frac{1}{1680\nu^7} \end{aligned}$$

$$\begin{aligned} V_8 &= \frac{z^2}{4096(1-z^2)^{12}\nu^8} (1024 + 248320z^2 + 5095936z^4 \\ &+ 24059968z^6 + 34280896z^8 + 15252048z^{10} \\ &+ 1765936z^{12} + 23797z^{14}) \end{aligned}$$

Hence we have actually increased Meissel's analysis by two orders. Using symbolic packages these orders were computed and higher terms should pose no problem if the application requires higher accuracy.

For the case when the argument is larger than the index, Meissel used the parametrization $z = \sec \beta$ [6], and we shall term it as his *Second* expansion. Hence,

$$J_\nu(\nu \sec \beta) = \sqrt{\frac{2 \cot \beta}{\nu \pi}} e^{-P_\nu} \cos \left(Q_\nu - \frac{1}{4} \pi \right) \quad (12)$$

where P_ν is given as,

$$P_\nu = P_1 + P_2 + P_3 + P_4 + \dots \quad (13)$$

where

$$P_1 = \frac{\cot^6 \beta}{16\nu^2} (4 \sec^2 \beta + \sec^4 \beta)$$

$$P_2 = -\frac{\cot^{12} \beta}{128\nu^4} (32 \sec^2 \beta + 288 \sec^4 \beta + 232 \sec^6 \beta + 13 \sec^8 \beta)$$

$$P_3 = \frac{\cot^{18} \beta}{192\nu^6} (48 \sec^2 \beta + 2580 \sec^4 \beta + 14884 \sec^6 \beta + 17493 \sec^8 \beta + 4242 \sec^{10} \beta + 103 \sec^{12} \beta)$$

$$\begin{aligned} P_4 &= \frac{\cot^{24} \beta \sec^2 \beta}{4096\nu^8} (1024 + 248320 \sec^2 \beta + 5095936 \sec^4 \beta \\ &+ 24059968 \sec^6 \beta + 34280896 \sec^8 \beta + 15252048 \sec^{10} \beta \\ &+ 1765936 \sec^{12} \beta + 23797 \sec^{14} \beta) \end{aligned}$$

and Q_ν is given as,

$$Q_\nu = Q_1 + Q_2 + Q_3 + Q_4 + \dots \quad (14)$$

and,

$$Q_1 = \nu(\tan \beta - \beta) - \frac{\cot^3 \beta}{24\nu} (2 + 3 \sec^2 \beta)$$

$$Q_2 = -\frac{\cot^9 \beta}{5760\nu^3} (16 - 1512 \sec^2 \beta - 3654 \sec^4 \beta - 375 \sec^6 \beta)$$

$$Q_3 = -\frac{\cot^{15} \beta}{322560\nu^5} (256 + 78720 \sec^2 \beta + 1891200 \sec^4 \beta + 4744640 \sec^6 \beta + 1914210 \sec^8 \beta + 67599 \sec^{10} \beta)$$

$$Q_4 = -\frac{\cot^{21} \beta}{3440640\nu^7} (881664 \sec^2 \beta + 99783936 \sec^4 \beta$$

$$+ 1135145088 \sec^6 \beta + 2884531440 \sec^8 \beta + 1965889800 \sec^{10} \beta + 318291750 \sec^{12} \beta + 5635995 \sec^{14} \beta - 2048)$$

It should be remarked that we disagree with Meissel's result for P_3 in the last four terms. However, we obtain perfect agreement with the rest of his results [6]. We have improved on his result by using V_7 , V_8 to obtain P_4 and Q_4 . Hence, we have increased the accuracy of this expansion by at least one order from Meissel's earlier result. Again, higher order results are easily obtainable and are available if needed.

In Figures 1 and 2 we have plotted these expansions in the regions they are expected to fail. These are the so called "transition" regions, where each expansion approaches a singularity (as the order equals the argument). For the computationally motivated (we can compute exact values of Bessel functions with ease) case of the $\nu = 300$, we note the following. Fig.1 indicates the onset of breakdown in the *First* expansion for argument values around and larger than 290. Similarly, Figure 2, indicates a similar breakdown starting around the values 300 and persisting till 310. Hence, the values outside these regions of breakdown or transition regions are well covered by Meissel's expansions. However, the issue as to deal with these regions need to be addressed via separate methods, which will be addressed in more detail in Section IV. The CPU time for these approximations was less than 0.01 seconds per value on a 2.4 GHz Pentium IV processor running MAPLE version 9. The "exact" MAPLE solver took somewhere between 0.03 to 0.08 seconds to compute each value. Clearly, there is a lot more computational speed in using a few terms present in these expansions. As an application, it should be noted that values of this order are applicable to the Peters-Mathews model of gravitational radiation from binary inspiralling stars [7].

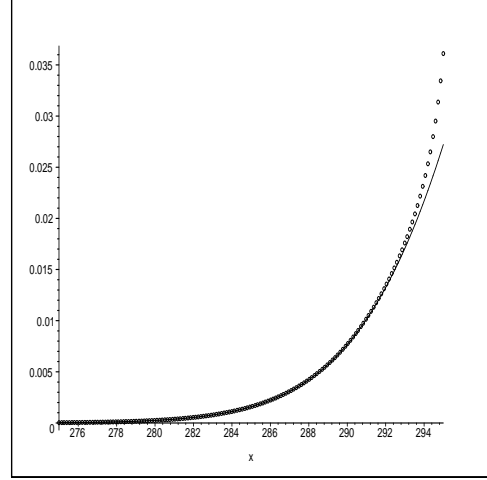


Figure 1: Meissel's *First* expansion and actual Bessel function graphed for argument x and order $\nu = 300$ near the transition region. Solid line indicates actual Bessel function values and circles indicate values given by the expansion.

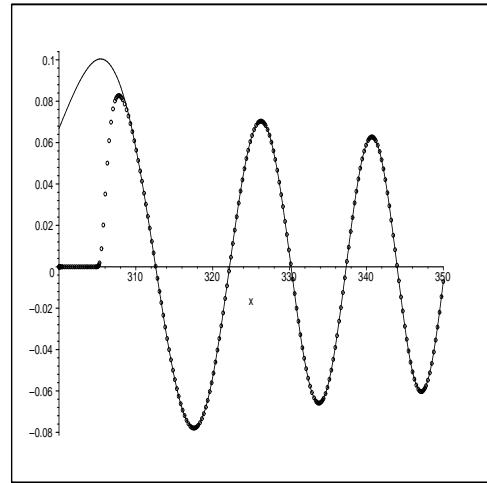


Figure 2: Meissel's *Second* expansion and actual Bessel function graphed for argument x and order $\nu = 300$ near the transition region. Solid line indicates actual Bessel function values and circles indicate values given by the expansion.

For the case when the argument equals the index, we extend Meissel's *Third* expansion [6] by two orders as follows:

$$J_n(n) \sim \frac{1}{\pi} \sum_{m=0}^{\infty} \lambda_m \Gamma\left(\frac{2m}{3} + \frac{4}{3}\right) \left(\frac{6}{n}\right)^{\frac{2}{3}m + \frac{1}{3}} \cos \pi\left(\frac{m}{3} + \frac{1}{6}\right) \quad (15)$$

where the terms, λ_m ($m = 0, 1, 2, \dots, 7$), are given by,

$$\begin{aligned} \lambda_0 &= 1, \lambda_1 = \frac{1}{60}, \lambda_2 = \frac{1}{1400}, \lambda_3 = \frac{1}{25200}, \\ \lambda_4 &= \frac{43}{17248000}, \lambda_5 = \frac{1213}{7207200000}, \lambda_6 = \frac{681563}{5721073600000}, \\ \lambda_7 &= \frac{63319}{7264857600000000} \end{aligned} \quad (16)$$

We observe that inclusion of the higher order terms leads to 10 decimal accuracy compared to actual values of large order Bessel functions.

The method of steepest descents was employed by Debye in [8]. For the case when the argument is less than the order, he obtained,

$$J_\nu(\nu \operatorname{sech}(\alpha)) \sim \frac{e^{\nu(\tanh \alpha - \alpha)}}{\sqrt{2\pi\nu \tanh \alpha}} \sum_{m=0}^{\infty} \frac{\Gamma(m + \frac{1}{2})}{\Gamma(\frac{1}{2})} \frac{A_m}{(\frac{1}{2}\nu \tanh \alpha)^m} \quad (17)$$

where,

$$\begin{aligned} A_0 &= 1, A_1 = \frac{1}{8} - \frac{5}{24} \coth^2 \alpha \\ A_2 &= \frac{3}{128} - \frac{77}{576} \coth^2 \alpha + \frac{385}{3456} \coth^4 \alpha \\ A_3 &= \frac{5}{1024} - \frac{1521}{25600} \coth^2 \alpha + \frac{17017}{138240} \coth^4 \alpha \\ &\quad - \frac{17017}{248832} \coth^6 \alpha \\ A_4 &= \frac{11513}{92897280} - \frac{21023}{9953280} \coth^2 \alpha + \frac{138919}{19906560} \coth^4 \alpha \\ &\quad - \frac{49049}{5971968} \coth^6 \alpha + \frac{230945}{71663616} \coth^8 \alpha \end{aligned}$$

Following this method, we have computed two higher orders A_3 and A_4 , using symbolic computation.

For the case when the argument is larger than the order, Debye obtains the following expansion:

$$J_\nu(\nu \sec \beta) \sim \sqrt{\frac{2}{\pi\nu \tan \beta}} \left[\cos\left(\nu \tan \beta - \nu\beta - \frac{1}{4}\beta\right) \right.$$

$$\begin{aligned} &\times \sum_{m=0}^{\infty} (-1)^m \frac{\Gamma(m + \frac{1}{2})}{\Gamma(\frac{1}{2})} \frac{A_{2m}}{(\frac{1}{2}\nu \tanh \alpha)^{2m}} + \sin(\nu \tan \beta) \\ &\left. - \nu\beta - \frac{1}{4}\beta\right) \sum_{m=0}^{\infty} (-1)^m \frac{\Gamma(2m + \frac{3}{2})}{\Gamma(\frac{1}{2})} \frac{A_{2m+1}}{(\frac{1}{2}\nu \tanh \alpha)^{2m+1}} \end{aligned} \quad (18)$$

where,

$$\begin{aligned} A_0 &= 1, A_1 = \frac{1}{8} + \frac{5}{24} \cot^2 \beta \\ A_2 &= \frac{3}{128} + \frac{77}{576} \cot^2 \beta + \frac{385}{3456} \cot^4 \beta \\ A_3 &= \frac{5}{1024} + \frac{1521}{25600} \cot^2 \beta + \frac{17017}{138240} \cot^4 \beta \\ &\quad + \frac{17017}{248832} \cot^6 \beta \\ A_4 &= \frac{11513}{92897280} + \frac{21023}{9953280} \cot^2 \beta + \frac{138919}{19906560} \cot^4 \beta \\ &\quad + \frac{49049}{5971968} \cot^6 \beta + \frac{230945}{71663616} \cot^8 \beta \end{aligned}$$

Again, we have extended Debye's result by two higher orders by obtaining A_3 and A_4 . However, due to the nature of this method we could not obtain reliable results that spanned in a generally predictable direction. Accuracy was limited to the region of the stationary phase as expected and hence, we recommend Meissel's expansions to be more reliable (except of course in the "transition" region) than the method of steepest descent.

4. Transitional regions: Contour Integration and extension of ϵ expansion

To address the issues related to computation for large order Bessel functions in the transition regions we present two methods that are geared to work in such domains. Firstly, we present the results by Watson, [5]. For the case of the argument being less than the order, he obtained via use of contour integration,

$$\begin{aligned} J_\nu(\nu \operatorname{sech}(\alpha)) &= \frac{\tanh \alpha}{\pi\sqrt{3}} \exp\left[\nu\left(\tanh \alpha + \frac{1}{3}\tanh^3 \alpha - \alpha\right)\right] \\ &\quad \times K_{\frac{1}{3}}\left(\frac{1}{3}\nu \tanh^3 \alpha\right) \\ &\quad + 3\theta_1 \nu^{-1} \exp[\nu(\tanh \alpha - \alpha)] \end{aligned} \quad (19)$$

where $\theta_1 < 1$. Similarly, for the case when the argument is greater than the order, he derived the following:

$$J_\nu(\nu \sec \beta) = \frac{1}{3} \tan \beta \cos\left[\nu\left(\tan \beta - \frac{1}{3}\tan^3 \beta - \beta\right)\right] \times$$

$$\left(J_{-\frac{1}{3}} + J_{\frac{1}{3}} \right) + 3^{-\frac{1}{2}} \tan \beta \sin \left[\nu \left(\tan \beta - \frac{1}{3} \tan^3 \beta - \beta \right) \right] \times \\ \left(J_{-\frac{1}{3}} - J_{\frac{1}{3}} \right) + 24\theta_2 \nu^{-1} \quad (20)$$

where $\theta_2 < 1$ and the argument for the Bessel functions $J_{\pm\frac{1}{3}}$ is $\frac{1}{3} \tan^3 \beta$. The great advantage of these formulae is that they have error bounds given. However, these extensions are not trivial as this involves solving extensions to Airy-type integrals, for which we do not presently have closed form answers. The other issue with these formulae is that they are themselves given in fractional Bessel function form which would pose computational problems once the arguments involved are large.

On the other hand, Debye [8], introduced, what we will term as “ ϵ expansion”. The idea is motivated by introducing a small parameter ϵ , such that $\nu = z(1 - \epsilon)$, where ν denotes the order and z is the argument of the Bessel function.

$$J_\nu(z) \sim \frac{1}{3\pi} \sum_{m=0}^{\infty} B_m(\epsilon z) \sin \frac{1}{3}(m+1)\pi \cdot \frac{\Gamma(\frac{1}{3}m + \frac{1}{3})}{(\frac{1}{6}z)^{\frac{1}{3}(m+1)}} \quad (21)$$

We have extended this analysis by 5 orders and the terms $B_m(\epsilon z)$, $m = 0, 1, 2, \dots, 15$, are given as,

$$B_0(\epsilon z) = 1, B_1(\epsilon z) = \epsilon z, B_3(\epsilon z) = \frac{1}{6}\epsilon^3 z^3 - \frac{1}{15}\epsilon z$$

$$B_4(\epsilon z) = \frac{1}{24}\epsilon^4 z^4 - \frac{1}{24}\epsilon^2 z^2 + \frac{1}{280}$$

$$B_6(\epsilon z) = \frac{1}{720} z^6 \epsilon^6 - \frac{7}{1440} z^4 \epsilon^4 + \frac{1}{288} z^2 \epsilon^2 - \frac{1}{3600} \quad (22)$$

$$B_7(\epsilon z) = \frac{1}{5040} z^7 \epsilon^7 - \frac{1}{900} z^5 \epsilon^5 + \frac{19}{12600} z^3 \epsilon^3 - \frac{13}{31500} z \epsilon$$

$$B_9(\epsilon z) = \frac{1}{362880} z^9 \epsilon^9 - \frac{1}{30240} z^7 \epsilon^7 + \frac{71}{604800} z^5 \epsilon^5 \\ - \frac{121}{907200} z^3 \epsilon^3 + \frac{7939}{232848000} z \epsilon$$

$$B_{10}(\epsilon z) = \frac{1}{3628800} z^{10} \epsilon^{10} - \frac{11}{2419200} z^8 \epsilon^8 + \frac{143}{6048000} z^6 \epsilon^6 \\ - \frac{803}{18144000} z^4 \epsilon^4 + \frac{43}{1728000} z^2 \epsilon^2 - \frac{1213}{655200000}$$

$$B_{12}(\epsilon z) = \frac{1}{479001600} z^{12} \epsilon^{12} - \frac{13}{217728000} z^{10} \epsilon^{10} + \\ \frac{11}{508032000} z^8 \epsilon^8 - \frac{377}{155520000} z^6 \epsilon^6 + \frac{337207}{83825280000} z^4 \epsilon^4 \\ - \frac{59503}{27941760000} z^2 \epsilon^2 + \frac{151439}{977961600000}$$

$$B_{13}(\epsilon z) = \frac{1}{6227020800} z^{13} \epsilon^{13} - \frac{1}{171072000} z^{11} \epsilon^{11} + \\ \frac{11}{145152000} z^9 \epsilon^9 - \frac{47}{108864000} z^7 \epsilon^7 + \frac{25853}{23950080000} z^5 \epsilon^5 \\ - \frac{266303}{259459200000} z^3 \epsilon^3 + \frac{169039}{698544000000} z \epsilon$$

$$B_{15}(\epsilon z) = \frac{1}{1307674368000} z^{15} \epsilon^{15} - \frac{1}{23351328000} z^{13} \epsilon^{13} \\ + \frac{113}{125737920000} z^{11} \epsilon^{11} - \frac{17}{1905120000} z^9 \epsilon^9 \\ + \frac{76841}{1760330880000} z^7 \epsilon^7 - \frac{37021}{371498400000} z^5 \epsilon^5 \\ + \frac{5141933}{57210753600000} z^3 \epsilon^3 - \frac{16720141}{810485676000000} z \epsilon$$

Terms B_{3m-1} , $m = 1, 2, \dots$ do not contribute in eqn. (21) due to the periodicity of the sine function. With symbolic computation, we are able to generate higher orders if needed.

To illustrate the applicability and issues of both these methods to the transition region, we present Figures 3 and 4, which are plotted for the problematic regions (when the order is $\nu = 300$) in Figures 1 and 2. Both methods show remarkable ability in capturing the functions in the domains of interest. In Figure 3, the ϵ expansion starts working at values at 286 and Watson’s formula works to even a larger domain. Similarly, in Figure 4, both the methods indicate success in regions where Meissel’s expansions fail. This starts at values of the argument, and works up to $x = 316$ for the ϵ expansion whereas, again, the domain of Watson’s formula is much greater. The reasons for lesser range of the ϵ expansion can be attributed to the fact that it is a power series compared to Watson’s formula which actually depends on fractional Bessel functions themselves. Further, the ϵ expansion depends crucially on the size of the parameter, which is connected with the order one is working with. However, the reason why we will persist with this method is that it will be more applicable when the argument of the Bessel function is quite large.

To illustrate the type of values a GW pulsar FT would require, we present Figures 5 and 6. Here, we choose a very large order (yet realistic phenomenologically) for the Bessel function, which is 1 million.

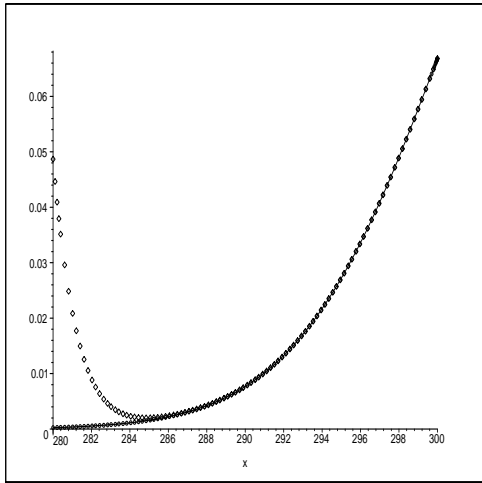


Figure 3: Comparison of ϵ expansion and Watson's formulae for argument $x < 300$ and order $\nu = 300$. Solid line indicates exact Bessel function values, diamonds represent ϵ expansion and circles indicate values given by Watson's formula.

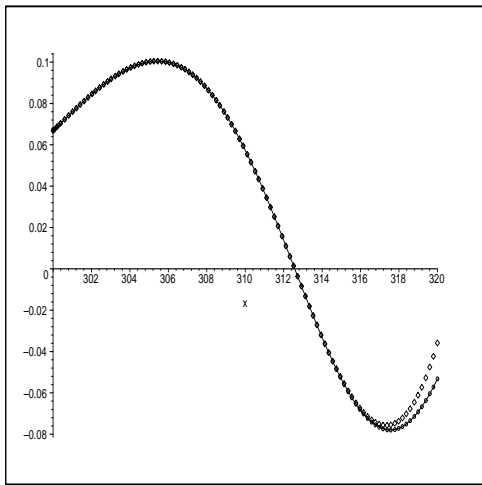


Figure 4: Comparison of ϵ expansion and Watson's formula in the transition region for argument $x > 300$ and order $\nu = 300$. Solid line indicates exact Bessel function values, diamonds represent ϵ expansion and circles indicate values given by Watson's formula.

Also, in such a scenario, we would be looking at values greater than one million, hence Meissel's second expansion along with the appropriate Watson's formula (eq. 20) will be put to use. We were not able to make exact comparison, obviously due to massive computer times required. In this regard, the problem of "exact" Bessel functions presents a genuine challenge to SHARCNET (Shared Hierarchical Academic Research Cluster Network) and HPC in general. In Figure 5, we observe strong evidence that the proposed asymptotic expansions are appropriate for GW signal analysis. Here, we note the transition region starting at values of the argument at 1,000,000 and going up to 1,000,200. In this region, both the ϵ expansion and Watson's formula almost coincide with each other. As usual, the ϵ expansion breaks down earlier, however, all three methods coincide in a certain region indicating that we have consistent methods that work for values relevant to GW analysis. Meissel's expansion is fairly easy to implement computationally and indicates good stability for rather large values of the argument. This is illustrated in Figure 6, where we plot this expansion for values ranging from 1,000,200 to 32,500,000, which are relevant for GW phenomenology. This appears as a black band and is a continuous function which indicates oscillations tightly bunched together. It is noteworthy that the method is stable and shows consistent behaviour over an extreme range of values for the argument. The CPU time consumed by each of the points, on the average took less than 0.01 seconds on MAPLE. The Bessel utility in MAPLE crashed repeatedly after 15-30 minutes on the same system described above. It should be remarked that Watson's formula lacks in this capacity as it depends on fractional Bessel functions itself, which will provide computational challenge for such values. A detailed analysis regarding computational advantage over exact computation will be addressed in a later work. It is aimed to not only address the question of GW analysis but will deal with general computational issues regarding large order Bessel functions.

5. Conclusion

In this present work, we have given an extended asymptotic analysis for the large order and argument Bessel functions. This analytically improves the earlier pioneering works of Meissel, Airey, Debye and Watson. These extensions should be of possible use not only in GW signal analysis, but also in a variety of problems in Engineering and the Sciences where the ubiquitous Bessel functions are encountered.

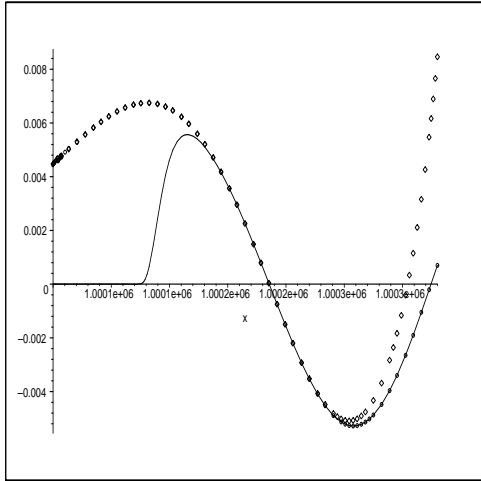


Figure 5: Comparison of Meissel's *Second* expansion, ϵ expansion and Watson's formulae for argument $x > 1,000,000$ and order $\nu = 1,000,000$. Solid line indicates Meissel's *Second* expansion values, diamonds represent ϵ expansion and circles indicate values given by Watson's formula.

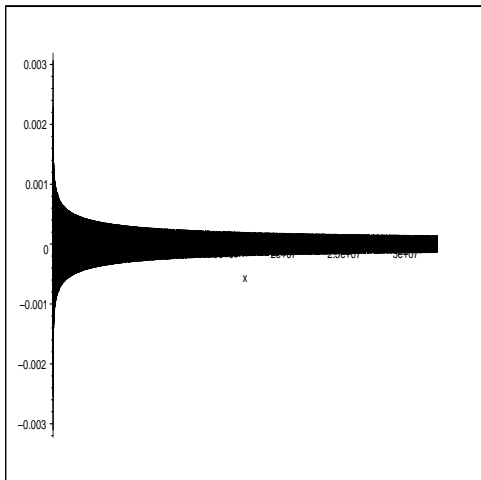


Figure 6: Plot of Meissel's *Second* expansion for argument, x ranging from 1,000,200 to 32,500,000 for order 1,000,000.

Acknowledgments

We are deeply grateful to SHARCNET for valuable grant support that made this study feasible. We are also indebted to Drs. Nico Temme (CWI, Amsterdam), Walter Gautschi (Purdue U.), D.G.C. McKeon (U. Western Ontario), Tom Prince (JPL, Pasadena) and the referee for valuable suggestions.

References

- [1] Kanti Jotania, S.R. Valluri and Sanjeev V. Dhurandhar, "A Study of the Gravitational Wave Form from Pulsars", *Astron. Astrophys.* vol. 306, pp. 317, 1996; S.R. Valluri, F.A. Chishtie, J.J. Drozd, R.G. Biggs, M.Davison, S. V. Dhurandhar and B.S. Sathyaprakash, "A study of the Gravitational Wave Form from Pulsars", *Class. Quant. Grav.* vol.19 pp. 1327-1334, 2002, Erratum-ibid. vol. 19, pp. 4227-4228, 2002.
- [2] MacPhie, R. H. and Wu, K.-L., "A Plane Wave Expansion of Spherical Wave Functions for Modal Analysis of Guided Wave Structures and Scatterers", *IEEE Trans. on Antennas and Propagation*, vol. 51, No. 10, pp. 2801-2805, 2003.
- [3] Thorne, K.S., "Multipole expansions of gravitational radiation", *Reviews of Modern Physics*, vol.52, pp. 299-339, 1980.
- [4] Allen, B. and Ottewill, A.C., *Detection of Anisotropies in the Gravitational-Wave Stochastic Background*, University of Wisconsin, and University College Dublin 1996.
- [5] Watson, G.N., *A treatise on the theory of Bessel Functions*, Cambridge University Press, 1958; *Proc. Camb. Phil. Soc.* vol. XIX, 96, 1918.
- [6] Meissel, D.F.E., "Neue Entwicklungen ueber die Bessel'schen Functionen" *Astr. Nach.* vol. CXXIX col. 281-284, 1892; *Astr. Nach.* vol. CXXX, "Weitere Entwicklungen ueber die Bessel'schen Functionen", col. 363-368, 1892; "Einige Entwicklungen die Bessel'schen I-Functionen betreffend" vol. CXXVII, col. 359-362, 1891; "Beitrag zur theorie der allgemeinen Bessel'schen Functionen" vol. CXXVIII (1891), col.145-154.
- [7] Peters P. C. and Mathews J., "Gravitational Radiation from Point Masses in a Keplerian Orbit", *Phys. Rev.* vol. 131, pp. 435-439, 1963; Barack, L. and Cutler, C., "LISA Capture Sources: Approximate Waveforms, Signal-to-Noise Ratios, and Parameter Estimation Accuracy" *Phys.Rev. D* vol. 69, 082005, 2004.
- [8] Debye, P., "Naeherungsformeln fuer die Zylinderfunktionen fuer grosse Werte des Arguments und unbeschraenkt veraenderliche Werte des Index", *Math. Ann.*, vol. LXVII pp.535-558, 1909.
- [9] Airey, J.R., "Bessel and Neumann Functions of Equal Order and Argument" *Phil. Mag.* (6) vol. XXXI, 520-528, 1916.